Strain and morphology of graphene membranes on responsive microhydrogel patterns

P. R. Shaina and Manu Jaiswal
Department of Physics, Indian Institute of Technology Madras, Chennai 600036, India

(Received 1 October 2014; accepted 3 November 2014; published online 11 November 2014)

We study the configuration of atomically-thin graphene membranes on tunable microhydrogel patterns. The polyethylene oxide microhydrogel structures patterned by electron-beam lithography show increase in height, with a persistent swelling ratio up to ~10, upon exposure to vapors of an organic solvent. We demonstrate that modifying the height fluctuations of the microhydrogel affects the strain and morphology of ultrathin graphene membrane over-layer. Raman spectroscopic investigations indicate that small lattice strains can be switched on in mechanically exfoliated few-layer graphene membranes that span these microhydrogel structures. In case of chemical-vapor deposited single-layer graphene, we observe Raman signatures of local depinning of the membranes upon swelling of microhydrogel pillars. We attribute this depinning transition to the competition between membrane-substrate adhesion energy and membrane strain energy, where the latter is tuned by hydrogel swelling. © *2014 AIP Publishing LLC*. [http://dx.doi.org/10.1063/1.4901746]

The morphology of a thin elastic membrane is determined by minimizing the sum of interfacial bonding energy, and system strain and bending energies.[1,2] Graphene, a monolayer of carbon atoms in honeycomb lattice structure, is a particularly interesting elastic sheet not only because it represents the truly two-dimensional (2D) limit but also because the morphology of graphene films strongly couples to its electronic degrees of freedom. Graphene membranes that are suspended across trenches show ultrahigh carrier mobility since the scattering rate from substrate impurities is suppressed.[1] The resistivity of graphene has important contributions from surface-phonon scattering from the substrate and from ripples within the graphene sheet; both these in turn depend on profile of the graphene sheet on the substrate.[3] Recently, an anomalous low-temperature transport in graphene has been related to a structural-phase transition of the underlying $SrTiO_3$ substrate.[3] For large uniaxial strains, a band-gap can be induced in the energy spectrum of graphene,[4,5] while giant pseudo-magnetic fields have been observed in strained graphene nanobubbles grown on metal substrates.[6,7] Graphene origami electronics has also been envisaged, with device elements derived from strain and morphology dependent electronic processes.[8] Practical realization of many theoretical propositions of strain-engineered graphene is non-trivial. Nonetheless, this has generated extensive interest in control of the nanoscale morphology of graphene.[9–11] The snap-through instability of graphene problem has also attracted recent attention, where by a partially depinned state of graphene has been proposed by appropriately engineered substrate patterns.[1,2]

In this paper, we demonstrate that microhydrogel patterns with tunable height fluctuations can serve as foundation for switching-on lattice strains and morphological transitions in graphene membranes on length scales amenable to lithographic fabrication. Thin layers of hydrogels on SiO_2/Si substrates are cross-linked with electron-beam exposure to form the microhydrogel patterns of desired lateral shape. We show that exposure to vapors of an organic solvent induces significant and persistent height change in the hydrogel patterns. This swelling generates strains in the over-layer comprising exfoliated few-layer graphene (FLG) membranes, which are measured as red-shifts in the Raman modes of graphene. In single-layer chemical-vapor deposited (CVD) graphene, swelling of microhydrogel pillars leads to partial depinning of the graphene membrane over-layer. This depinning is observed locally on graphene membranes spanning across biaxially strained microhydrogel pillars, and its signature is manifest in the suppression of electron or hole inelastic scattering rate for the 2D Raman mode.

Hydrogels are water-soluble polymers which swell upon absorbing organic solvents and ionic aqueous solutions. Here, polyethylene oxide (PEO) (M.W. 100 K, Alfa Aesar) is used as the polymeric hydrogel. PEO films are prepared by spin-coating 1 wt. % aqueous solution on SiO_2/Si wafers. The cross-linked PEO patterns are made using electron-beam lithography with an optimized dose of 50 μC/cm^2. While exfoliated FLG is introduced as an over-layer prior to patterning, CVD graphene is wet transferred post-patterning on the microhydrogel layer. This is necessary because the un-patterned polymer is soluble in water and therefore, not amenable to a wet transfer process required for CVD graphene. Large-area CVD films allow experiments with single-layer graphene (SLG) since the roughness of polymer film together with the poor optical contrast of graphene on the PEO/SiO_2/Si hetero-structure limits the options of using mechanical exfoliation for SLG.

Figure 1(a) shows the optical image of microhydrogel pillars of radius 1.5 μm taken using a 3D non-contact optical profilometer (Bruker) with height 12 ± 1 nm. Figure 1(b) shows the scanning electron microscope (SEM) image of 0.5 μm radius microhydrogel pillars on SiO_2/Si substrate. For this work, circular microhydrogel pillars are patterned, having radius 0.1–1.5 μm. In addition, large-area pads (50 μm side) and other structures are also fabricated for the study. The choice of patterns is based on the type of strain that could potentially be induced in the graphene over-layer.

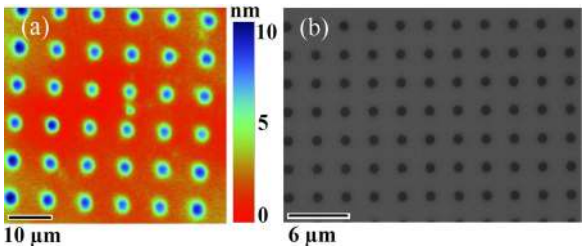

FIG. 1. Microhydrogel pillars on SiO_2/Si substrate: (a) 2D optical profile image; (b) SEM image.

Now, we consider the influence of several solvents on the swelling of cross-linked microhydrogels. A representative pattern comprising of an array of 5 μm wide rectangular pads separated by 10 μm gap is used for this study. Figure 2(a) shows the height change measured using optical profilometry, induced on the polymer pillars before and after solvent vapor exposure. Microhydrogel PEO is known to swell upon immersing in water with a swelling ratio up to 14–16.[12] However, the swelling does not persist when the samples are removed from water. Exposure to vapors of water and organic solvents including toluene, isopropyl alcohol (IPA), anisole, methyl isobutyl ketone (MIBK) as well as ethyl-2-cyanoacrylate (Sigma Aldrich) are used to swell the microhydrogel patterns. From Figure 2(a), it is evident that the persistent height changes produced by most solvents are substantially less than that produced by cyanoacrylate (henceforth called as CA-1) vapors. CA-1 vapors result in microhydrogel swell from 12 ± 1 nm to 74 ± 4 nm. In addition, exposure to vapors of a readily available cyanoacrylate-based commercial adhesive Fevikwik (Pidilite®; henceforth called as CA-2) results in further enhanced persistent swelling ratio of ~10, with a final height of 111 ± 5 nm. Figure 2(b) shows the dependence of microhydrogel swelling ratio on the initial extent of electron-beam induced cross-linking, and values ranging from 3.9 to 6.5 are obtained by changing the electron-beam dose. Thus, exposure to CA vapors can be used to generate widely tunable height fluctuations over a given lateral length scale in the patterned substrates that act as an under-layer for graphene membranes.

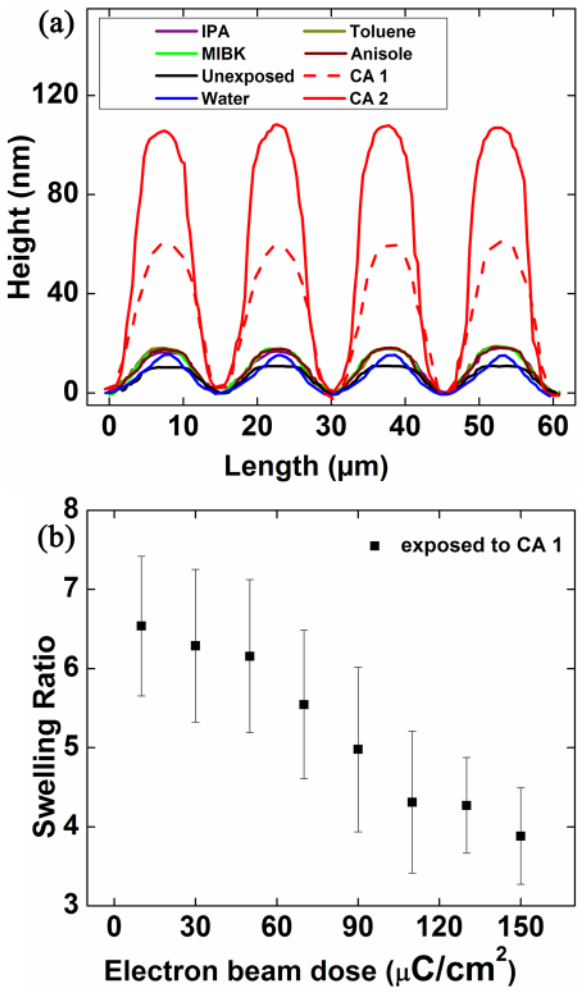

FIG. 2. (a) Height change of microhydrogel patterns upon exposure to vapors of several solvents. (b) Swelling ratio versus electron-beam dose.

We next consider the effect of microhydrogel pillar height changes on the graphene over-layer. We use micro-Raman spectroscopy (Horiba HR-800-UV) to study the effect of change in height fluctuations of the substrate pattern on the strain and morphology of the graphene over-layer. Raman measurements are done in ambient conditions using $\lambda = 632.8$ nm from a He-Ne laser while the Raman maps are generated using $\lambda = 532$ nm from a semiconductor-diode laser. Figure 3 shows the G and 2D Raman bands of FLG (sample S3) before and after microhydrogel swelling. The G and 2D peaks are red-shifted from the original position after swelling of the microhydrogels, with $\Delta\omega_G = 8\,cm^{-1}$ and $\Delta\omega_{2D} = 15.7\,cm^{-1}$. The inset shows the shifts for 6 FLG samples which give an average shift of $5.57 \pm 1.74\,cm^{-1}$ and $10.13 \pm 3.82\,cm^{-1}$ for G and 2D band peak positions, respectively. The shift in Raman peak positions could, in principle, arise from (a) Fermi-level shifts in graphene sheet,[13] (b) thermal effects,[14] or (c) lattice strain induced by swelling of microhydrogel under-layer.[13] We first look into the possibility of Fermi-level shift. For the case of SLG, a stiffening or blue-shift of the G-band frequency upon hole or electron doping up to 0.8 eV is well known.[13] This is quite opposed to the red-shifts in ω_G and ω_{2D}, which are experimentally observed in our samples. Furthermore, SLG and

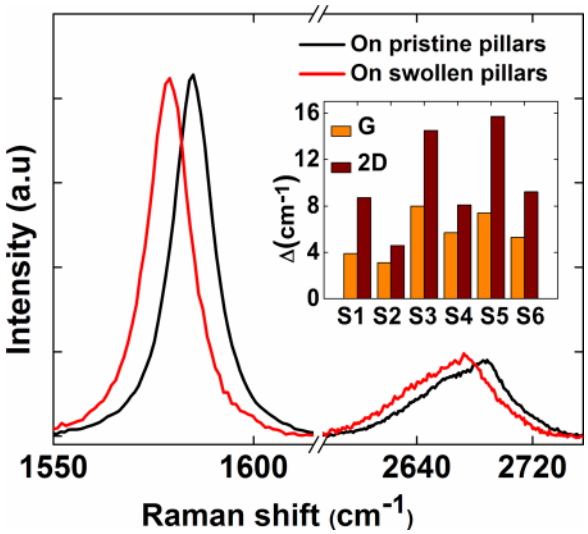

FIG. 3. Raman spectra of FLG showing red-shifts of G and 2D- band peaks after swelling of microhydrogel pillars [Inset: $\Delta\omega_G$ and $\Delta\omega_{2D}$ for 6 samples.]

FLG samples, which are exfoliated directly on SiO_2/Si substrate and exposed to CA vapors under identical conditions, show negligibly small Raman shifts, thereby ruling out the possibility that the solvent vapors are doping the graphene sheet. The peak positions of 2D and G bands can also vary with increase in the temperature of the lattice.[14] The FLG samples on microhydrogel pillars measured with laser intensities varying from 0.07 mW to 7 mW also show negligible change in Raman peak positions. Finally, we consider the third possibility of lattice strain in FLG. Based on purely geometrical considerations, the swelling of microhydrogel pillars can be expected to induce biaxial strain from expansion of the graphene lattice. Grüneisen parameters determine the Raman shift for a given magnitude and profile of lattice strain.[13] The values of Grüneisen parameters of FLG for ω_G and ω_{2D} have been experimentally reported under compressive biaxial strain using *in-situ* high pressure Raman spectroscopy.[15] The value of biaxial strain can be obtained independently from the ω_G and ω_{2D} position shifts. The strain estimated in FLG from G-band shift is $0.199 \pm 0.036\%$ and the value from 2D band shift is $0.181 \pm 0.006\%$ for sample S3. Comparable ratios of $\Delta\omega_{2D}/\Delta\omega_G$ are obtained for all FLG samples. Therefore, it is reasonable to attribute the observed red-shifts to lattice strain in graphene. The strain profile of FLG induced by the vertical swelling of microhydrogel pillars is well described by biaxially strained expanding lattice.

Now, we examine the response of single-layer graphene (SLG) samples to swelling of microhydrogel pillars. The Raman spectra of a representative SLG sample (M1) before and after swelling of microhydrogel pillar is shown in Figure 4(a). A red-shift of $4.4\,cm^{-1}$ is observed for G peak and $8.9\,cm^{-1}$ for 2D peak; the ratio of the shifts once again suggests a biaxial strain in SLG. However, the more prominent change in the Raman spectrum is the enhancement of the ratio of the integrated intensity of 2D to G bands, I_{2D}/I_G from 3.27 to 13.7, subsequent to swelling of the microhydrogel. We next look at the factors that could cause such a large I_{2D}/I_G ratio. A large value of I_{2D}/I_G can potentially arise from (i) interference enhancement effect associated with the multiple-reflections from the substrate layers[16] or (ii) suppression of electron or hole inelastic scattering rate associated with the underlying substrate.[17] Figure 4(b) shows Raman map of I_{2D}/I_G ratio for SLG spanning a microhydrogel pillar subsequent to CA vapor exposure (sample M2). Enhancement in the I_{2D}/I_G value beyond 10 is once again observed that is locally limited over a few regions around the pillar of 0.5 μm radius and even extending into the SiO_2/Si substrate region. Figure 4(c) shows a Raman map of I_{2D}/I_G ratio for SLG membrane that spans over a microhydrogel step feature of identical height. In this case, the value is limited to $I_{2D}/I_G < 7$ everywhere. These results suggest that large values of I_{2D}/I_G do not depend on the thickness of polymer layers alone as would be expected from an interference related process, but the pattern geometry plays an important role. To examine this second possibility in detail, a statistically large number ($N = 40$) of SLG samples on several polymer microhydrogel structures (small radius pillars with $r = 0.1$ to 1.5 μm and on large-area pads of side 50 μm of size) are measured. Figure 4(d) shows a plot of the I_{2D}/I_G ratio (before) versus I_{2D}/I_G (after) the swelling of microhydrogel pillars for these samples. Two types of samples are present: (A) $I_{2D}/I_G < 9$, both before and after swelling of microhydrogel: these comprise graphene on all large-area pads and also on some pillars, (B) $I_{2D}/I_G \sim 10$ to 16 observed for graphene on microhydrogel pillars alone, subsequent to their swelling. When considered together, these results indicate that thickness-dependent interference related signal enhancement cannot explain the large values of I_{2D}/I_G ratio for graphene on several pillars and also their absence from pads of identical heights. A large I_{2D}/I_G ratio can arise from the suppression of the inelastic scattering rate which is relevant only for the double-resonant 2D band and

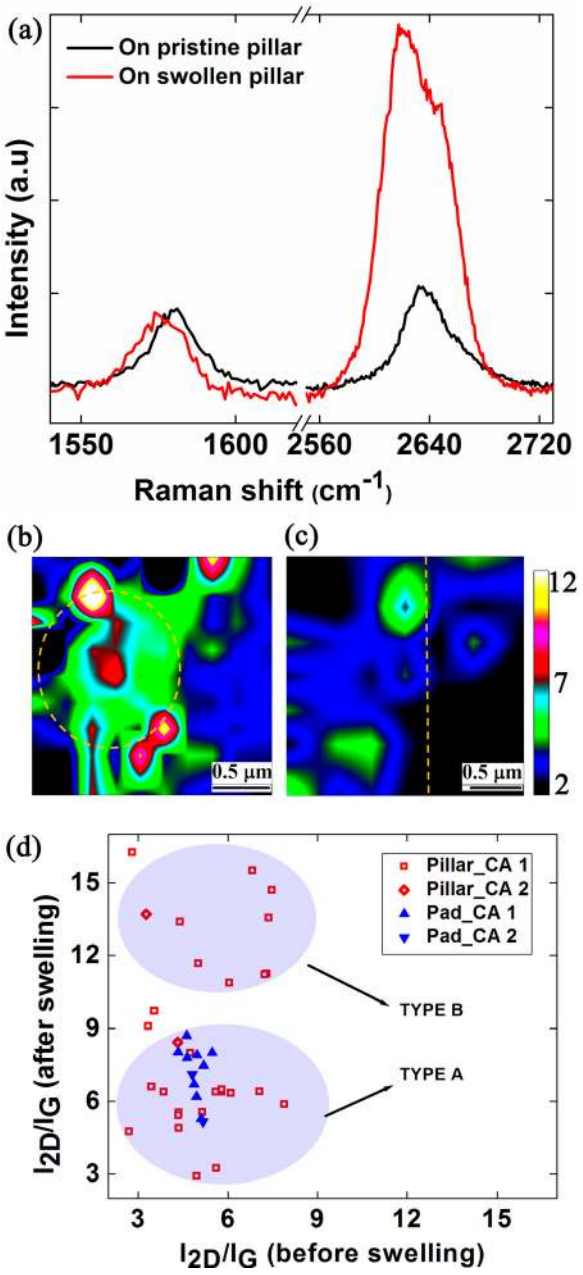

FIG. 4. (a) Intensity versus Raman shift for SLG before and after swelling of microhydrogel pillars. Spectra are normalized to the integrated intensity of the G mode. (b) Raman map of integrated I_{2D}/I_G intensity for SLG spanning a pillar of radius 0.5 μm, subsequent to swelling. (c) Raman map of integrated I_{2D}/I_G intensity for SLG spanning a step feature, subsequent to swelling [*Dashed yellow lines define approximate position of the pillar and step*.]. (d) I_{2D}/I_G of SLG on different substrate patterns before and after swelling of microhydrogels.

not for the G-band.[17] The physical situation where I_{2D}/I_G ratio takes on values as high as 10–16 is that of graphene suspended across a trench.[16–18] Interestingly, a partial depinning or detachment of graphene membrane is also possible on a patterned substrate, and this problem of the snap-through instability of graphene has been analytically investigated.[1,2] The interaction of graphene with the hydrogel substrate is important in determining its ability to conform to the shape of the pattern. This interaction primarily comprises electrostatic forces arising from polar modes and charged impurities of the substrate, but also includes some contributions from van der Waals forces.[19] Chemical modification or bond formation at the graphene surface is not involved.[19,20] The depinning transition of graphene membrane from the underlying patterned substrate can occur when the graphene-substrate adhesion energy is insufficient to compensate for the strain energetic costs required for graphene to conform to the shape of the pattern. In such cases, graphene membranes can locally relax strain by depinning from the substrate. In the above analytical studies, the depinning transition for graphene on bumps depends on a parameter defined by the ratio of bump-height (s) to a lateral length scale (l), as well as the interfacial bonding parameter. An increase in the ratio s/l beyond values of the order 0.1 can partially depin graphene for a graphene-substrate interaction energy per unit area of the order $1\,\mathrm{meV\AA^{-2}}$, which corresponds to electrostatic forces.[1,19] In our experiments, the swelling of microhydrogel pillars typically changes s/l from $\sim$0.01 to $\sim$0.1. The fact that depinning is not observed on all pillars may stem from the local nature of the phenomena, though other factors that can relax strain (tear or crack during processing) may also be responsible. We suggest that the enhanced I_{2D}/I_G intensity up to values $\sim$16 on swollen polymer microhydrogel pillars results from a partial depinning transition of the graphene membranes on these patterns.

In conclusion, we have studied the substrate regulated strain and morphology of graphene membranes spanning lithographically patterned microhydrogels which have substantially controllable height fluctuations. Biaxial strain is observed on graphene over-layers when the microhydrogel pillars swell vertically by a factor up to 10, in response to an organic vapor exposure. Furthermore, the variations of height with respect to the lateral length scale of the patterns allow single-layer graphene membranes to be partially depinned on top of the patterned substrate. This concept of using responsive resist patterns as knobs to tune strains in membrane overlayers can also be extended to other interfacial systems.

This work was supported by DST Grant No. FTP/PS-072/2012, DAE YSRA Grant No. 2012/20/37P/10/BRNS, Nissan NRSP, and IIT-M NFSC. The use of facilities at CNNP, IIT-M, and CenSE, IISc. is acknowledged.

[1]S. V. Kusminskiy, D. K. Campbell, A. H. C. Neto, and F. Guinea, Phys. Rev. B **83**, 165405 (2011).
[2]T. Li and Z. Zhang, Nanoscale Res. Lett. **5**, 169 (2010).
[3]S. Saha, O. Kahya, M. Jaiswal, A. Srivastava, A. Annadi, J. Balakrishnan, A. Pachoud, C. T. Toh, B. H. Hong, J. H. Ahn, T. Venkatesan, and B. Özyilmaz, Sci. Rep. **4**, 6173 (2014).
[4]V. M. Pereira and A. H. C. Neto, Phys. Rev. B **80**, 045401 (2009).
[5]S. M. Choi, S. H. Jhi, and Y. W. Son, Phys. Rev. B **81**, 081407(R) (2010).
[6]N. Levy, S. A. Burke, K. L. Meaker, M. Panlasigui, A. Zettl, F. Guinea, A. H. C. Neto, and M. F. Crommie, Science **329**, 544 (2010).
[7]J. Lu, A. H. C. Neto, and K. P. Loh, Nat. Commun. **3**, 823 (2012).
[8]V. M. Pereira and A. H. C. Neto, Phys. Rev. Lett. **103**, 046801 (2009).
[9]T. M. G. Mohiuddin, A. Lombardo, R. R. Nair, A. Bonetti, G. Savini, R. Jalil, N. Bonini, D. M. Basko, C. Galiotis, N. Marzari, K. S. Novoselov, A. K. Geim, and A. C. Ferrari, Phys. Rev. B **79**, 205433 (2009).
[10]J. Zabel, R. R. Nair, A. Ott, T. Georgiou, A. K. Geim, K. S. Novoselov, and C. Casiraghi, Nano Lett. **12**, 617 (2012).
[11]C. Metzger, S. Rémi, M. Liu, S. V. Kusminskiy, A. H. C. Neto, A. K. Swan, and B. B. Goldberg, Nano Lett. **10**, 6 (2010).
[12]P. Krsko, S. Sukhishvili, M. Mansfield, R. Clancy, and M. Libera, Langmuir **19**, 5618 (2003).
[13]A. Jorio, R. Saito, G. Dresselhaus, and M. S. Dresselhaus, *Raman Spectroscopy in Graphene Related Systems* (Wiley-VCH Verlag GmbH & Co. KGaA, Weinheim, Germany, 2011).
[14]S. Ghosh, W. Bao, D. L. Nika, S. Subrina, E. P. Pokatilov, C. N. Lau, and A. A. Balandin, Nat. Mater. **9**, 555 (2010).
[15]J. E. Proctor, E. Gregoryanz, K. S. Novoselov, M. Lotya, J. N. Coleman, and M. P. Halsall, Phys. Rev. B **80**, 073408 (2009).
[16]L. Wang, Z. Chen, C. R. Dean, T. Taniguchi, K. Watanabe, L. E. Brus, and J. Hone, ACS Nano **6**(10), 9314 (2012).
[17]Z. H. Ni, T. Yu, Z. Q. Luo, Y. Y. Wang, L. Liu, C. P. Wong, J. Miao, W. Huang, and Z. X. Shen, ACS Nano **3**(3) 569 (2009).
[18]S. Berciaud, S. Ryu, L. E. Brus, and T. F. Heinz, Nano Lett. **9**(1), 346 (2009).
[19]J. Sabio, C. Seoánez, S. Fratini, F. Guinea, A. H. C. Neto, and F. Sols, Phys. Rev. B **77**, 195409 (2008).
[20]S. Garg, B. Singh, X. Liu, A. Jain, N. Ravishankar, L. Interrante, and G. Ramanath, J. Phys. Chem. Lett. **1**, 336 (2010).